Multirate Optical Fast Frequency Hopping CDMA System Using Power Control

Elie Inaty, *Student Member, IEEE*, Hossam M. H. Shalaby, *Senior Member, IEEE*, Paul Fortier, *Senior Member, IEEE*, and Leslie A. Rusch, *Senior Member, IEEE*

***Abstract*—This paper addresses the problem of real-time multimedia transmission in fiber-optic networks using code division multiple access (CDMA). We present a multirate optical fast frequency hopping CDMA (OFFH-CDMA) system architecture using fiber Bragg gratings (FBGs). In addition, we argue that, in multimedia applications, different services have different quality of service (QoS) requirements; hence, the user only needs to use the minimum required power to transmit the signal, such that the required signal-to-interference ratio (SIR) is met. We show that a variable bit rate optical communication system with variable QoS can be implemented by way of power control with great efficiency. Present-day multirate optical CDMA systems concentrate on finding the code structure that supports a variable rate system, neglecting the importance of the transmission power of active users on the multiple access interference (MAI) and, therefore, on the system capacity. In this work, we assign different power levels to each rate through a power control algorithm using variable optical attenuators, which minimizes the interference and, at the same time, provides variable QoS constraints for different traffic types. Although we are using a code family that preserves good correlation properties between codes of different lengths, simulations show a great improvement in the system capacity when power control is used.**

***Index Terms*—Fiber Bragg grating (FBG), multimedia network, multirate optical frequency hopping code division multiple access (OFFH-CDMA), power control function.**

I. Introduction

THE subject of integration of heterogeneous traffic in optical code division multiple access (CDMA) has received much attention lately [3], [4]. This is due to growing interest in the development of broad-band optical fiber communication networks for multimedia applications. Future networks are required to accommodate a variety of services, including multirate data, graphics, audio, video, voice, and image with different performance and traffic constraints. Each type requires a given quality of service (QoS) specified by its signal-to-interference (SIR) ratio. For example, voice terminals have stringent delay requirements but tolerate some transmission errors, whereas errors cannot be tolerated at the destination for high-speed data transfer [1]. Moreover, real-time video communications require both error-free transmission and real-time delivery [2].

Previous works have addressed multirate communication using optical direct sequence CDMA (DS-CDMA) [2], [3]. In these works, the strategy has largely been to give priority to the code structure that supports multirate traffic. Although the code family plays an important role in the performance of a communication system, it is not the only factor to be considered in the analysis and design of a multirate optical CDMA system. This is especially true when the system allows users to dynamically switch traffic types for different connection applications with different QoS requirements. Even when using a code family that supports multirate applications and preserves auto- and cross-correlation properties between codes of different lengths, higher rate users exhibit low performance compared to lower rate users. This will limit the number of higher rate users, especially if they require high QoS, as is the case for high-speed data transfer. We will prove that by controlling the optical transmission power of each rate, using variable optical attenuators, we are able to reduce the wide differences between bit error rates (BERs) for different types of traffic, therefore helping to meet QoS requirements.

It must be noted that a sort of power control was proposed previously for single-rate DS-CDMA systems by using double optical hard-limiter correlation receivers [4]. This technique needs two threshold settings for the first and second hard limiters. These thresholds are generally dependent on the received optical power and the number of simultaneous users. Furthermore, optical hard limiters with variable thresholds do not exist in practice. For this reason, we propose to limit the interference directly from the transmitter using variable optical attenuators; thus, the receiver will remain a simple optical correlator.

In Section II, we propose a multirate optical fast frequency hopping CDMA (OFFH-CDMA) [5] system based on a power control algorithm that maximizes the system capacity and, at the same time, allows dynamic switching of traffic rates. We present a possible implementation of multirate OFFH-CDMA encode–decoder. Performance analysis and simulation results for a dual-rate communication scenario are investigated in terms of BER with and without power control in Section III. Section IV presents an upper bound on the system capacity based on the QoS requirements that are specified by lower bounds on the SIR. In Section V, we are able to optimize the power control function by solving a nonlinear programming problem using linear programming theory based on which a newly defined function is derived. This function enables us to obtain an analytical solution to the optimal power function that maximizes the system throughput. In addition, insightful simulations and discussions are presented in Section VI. Finally, our conclusion is given in Section VII.

Manuscript received October 27, 2000; revised October 24, 2001.

The authors are with the Department of Electrical and Computer Engineering, Laval University, Québec, QC G1K 7P4, Canada (e-mail: inati@gel.ulaval.ca; shalaby@ieee.org; fortier@gel.ulaval.ca; rusch@gel.ulaval.ca).

Publisher Item Identifier S 0733-8724(02)00142-1.

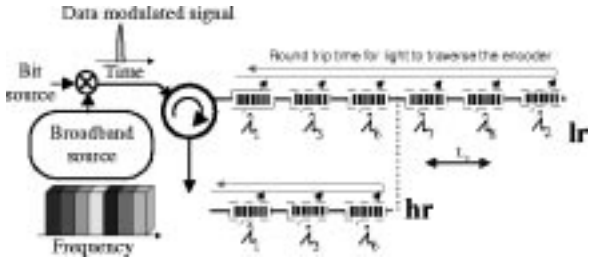

Fig. 1. Multirate OFFH-CDMA system.

II. Multirate OFFH-CDMA With Power Control

Optical FFH-CDMA has been proposed in [5]. The encoding and decoding are achieved passively using a sequence of fiber Bragg gratings (FBGs). The gratings will spectrally and temporally slice an incoming broad-band pulse into several components [6], as shown in Fig. 1 (encoder lr). Pulses are equally spaced at chip intervals T_c seconds apart, corresponding to the round-trip propagation time between two consecutive gratings. The chip time is given by $T_c = 2n_gL_c/c$. L_c represents the sum of one grating length and one spacing distance between adjacent grating pairs, c is the speed of light, and n_g is the group index. The time spacing, the chip duration, and the number of gratings will limit the data bit rate of the system, i.e., all reflected pulses should exit the fiber before the next bit enters. The bit duration is given by the total round-trip time in a grating structure of N gratings, $T = 2(N-1)n_gL_c/c$, where N is referred to as the *processing gain* (PG $= N$).

A. Programmable Multirate OFFH-CDMA Encoder–Decoder Device

It is important to emphasize the difference between passive optical CDMA and its electrical active counterpart in order to justify our work. In fact, in active CDMA systems, there is a one-to-one correspondence between the transmitted symbol duration and the PG in the sense that changing the bit duration will eventually lead to a change in the user's PG. On the other hand, this one-to-one relation does not exists in passive optical CDMA systems. For instance, decreasing the bit duration will not affect the symbol duration at the output of the optical encoder. Therefore, for a fixed PG, increasing the link transmission rate beyond a given value, known as the nominal rate, leads to bit overlap at the output of the encoder [7]. This, in turn, leads to high interference level. The idea is to respect the total round-trip time for light from a data bit to traverse the encoder. Our intention is to guarantee the one-to-one correspondence between the PG and the source transmission rate. Therefore, in order to increase the transmission rate, we should decrease the duration of the total round-trip time for light to go through the encoder–decoder and, hence, decrease the code duration. Given these constraints, it is clear that we are naturally using fixed chip rate and variable PG to achieve a multirate system. As a result, in order to dynamically control the spreading gain of an OFFH-CDMA user, we should control the length of the code of this user represented by the PG. Fig. 1 shows an illustrative example of a lower (lr) and higher (hr) rate encoder structure. In Fig. 2, we show the frequency hopping patterns corresponding to the lower and higher rate cases presented in Fig. 1. Programmability or multirate reconfigurability of the encoder–decoder is possible using tunable FBGs. In fact, in order to obtain shorter codes, wavelengths from longer codes can be tuned outside the working bandwidth of the system. In doing so, these wavelengths are no longer reflected by the intended encoder–decoder; hence, the reflected pattern looks like the one presented in Fig. 2(b). It is important to mention that the limitation on the multirate reconfigurability of the system is related to the tunability margin of the fiber Bragg grating [5].

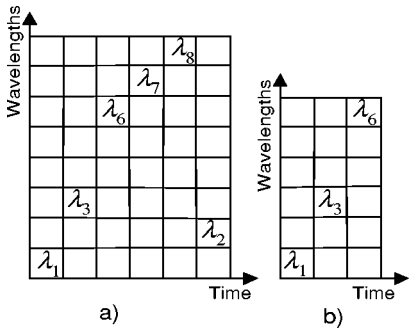

Fig. 2. FFH Pattern for (a) lower rate and (b) higher rate users.

Due to the fact that the weight for a higher rate user is less than that for lower rate users, dramatic decrease in the higher rate SIR will be experienced; hence, low performance can be expected.

B. Proposed Communication System

Consider a fiber-optic CDMA communication network with transmitter–receiver pairs using OFFH-CDMA with ON-OFF keying modulation. This system supports K users, which share the same optical medium in a star architecture, as shown in Fig. 3. Each of the K users has the possibility of switching its traffic rate for any of S possible values $R_1 < R_2 < \ldots < R_S$ corresponding to S different types of multimedia traffic or S different classes[1] . Each of these classes is constrained to a given QoS $\in \{\text{QoS}_1, \text{QoS}_2, \ldots, \text{QoS}_S\}$ requirement. The corresponding PGs are given by $N_1 > N_2 > \ldots > N_S$. Furthermore, a power control block is used in order to limit the interference and optimize the system capacity. In fact, this can be easily implemented using variable optical attenuators. Accordingly, we must determine the function $P^{(s)}$ that represents the transmission power of users transmitting at rate $R_s \in \{R_1, R_2, \ldots, R_S\}$. $P^{(s)}$ is given in (1), where we define $0 < \alpha_s \leq 1$ to be its corresponding attenuation function. We assume all users transmitting at the same rate will have the same level of attenuation. P represents the maximum power available in the system

$$P^{(s)} = \alpha_s P \quad \text{with } s \in \{1, 2, \ldots, S\}. \tag{1}$$

III. Performance Analysis

A. Hamming Auto- and Cross-Correlation

In frequency hopping CDMA systems, mutual interference occurs when two or more transmitters use the same frequency

[1]In this paper, rate and class are used interchangeably.

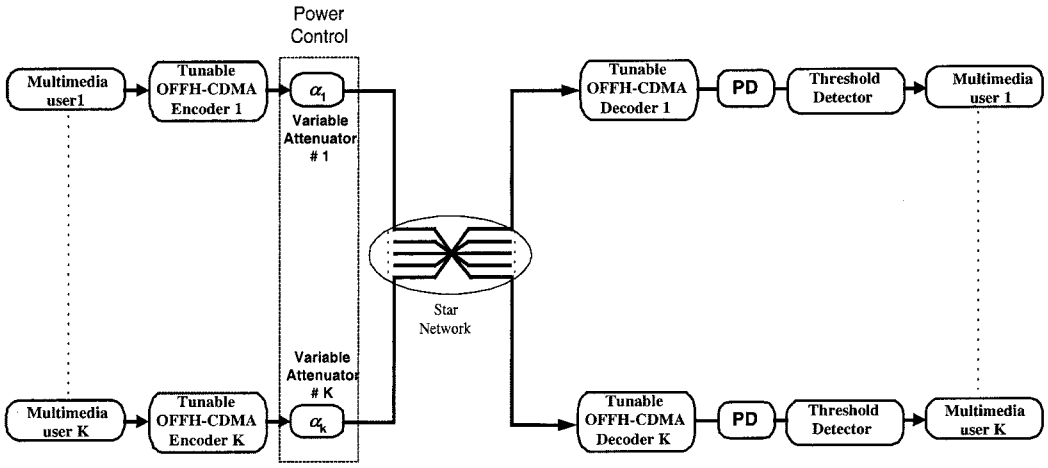

Fig. 3. Block diagram of the proposed OFFH-CDMA network for multimedia communication.

at the same time. This interference can be controlled by the cross correlation of the frequency hopping sequences. One of the best hopping sequence performance measures is provided by the periodic Hamming cross-correlation function $H_{XY}(\ )$ [8]. Let $X = [X(0), X(1), \ldots, X(N_{S1}-1)]$ and $Y = [Y(0), Y(1), \ldots, Y(N_{S2}-1)]$ denote two hopping sequences of periods N_{S1} and N_{S2}, respectively, with $N_{S1} < N_{S2}$. Let $X(l)$ and $Y(l) \in \{f_1, f_2, \ldots, f_q\}$, where f_i is one of the q possible frequency slots. Suppose that X is the desired user's code and Y is the interferer code. At the receiver, the Hamming cross correlation between these two sequences is defined as

$$H_{X,Y}(\tau) = \sum_{i=0}^{N_{S1}-1} h(X(i), Y(i-\tau)), \quad \text{for} -N_{S2}+1 \le \tau \le N_{S1}-1 \quad (2)$$

where the sum $(i-\tau)$ is taken modulo N_{S1} and $h(\cdot)$[2] is the Hamming function. The autocorrelation function is defined as

$$H_{X,X}(\tau) = \sum_{i=0}^{N_{S1}-1} h(X(i), X(i-\tau)) \quad \text{for } -N_{S1}+1 \le \tau \le N_{S1}-1. \quad (3)$$

The average variance of the cross correlation between two users transmitting at rates R_{S1} and R_{S2}, and using codes X and Y, is given by

$$\sigma^2_{X,Y} = \frac{1}{N_{S2}+N_{S1}-1} \sum_{\tau=-N_{S2}+1}^{N_{S1}-1} (H_{X,Y}(\tau) - \bar{H}_{X,Y}(\tau))^2 \quad (4)$$

where $\bar{H}_{X,Y}(\tau)$ is the delay-averaged value of the cross-correlation function.

B. SIR

In this paper, the SIR experienced by users clustered in each class plays an important role in determining the performance of these users, and, therefore, the system capacity. Each class $j \in \{1, 2, \ldots, S\}$ is characterized by its own QoS requirement, specified by a given SIR_j. Hence, the SIR experienced by an active user that has rate R_j, where $j \in \{1, 2, \ldots, S\}$ [3], is

$$\text{SIR}_j = \frac{N_j^2}{(K_j-1)\sigma^2_{j,j} + \sum_{\substack{s=1 \\ s\neq j}}^{S} K_s \frac{\alpha_s}{\alpha_j}\sigma^2_{j,s} + (\sigma_n^2)'} \quad (5)$$

where

$$K = \sum_{s=0}^{S-1} K_s$$

N_j, α_j and K_j are the PG, the attenuation value, and the number of active users in *class* j, respectively. $\sigma^2_{j,j}$ and $\sigma^2_{j,s}$ are the average variances of the cross-correlation amplitude in the same class and between different classes, respectively. In addition, $(\sigma_n^2)'$ represents the additive white Gaussian noise (AWGN) power spectral density after power control.

C. BER

Using the Gaussian assumption for multiple access interference (MAI) [9] and equiprobable data, the probability of error (or the BER), for each class of users is given by

$$P_e^{(j)} = Q\left(\sqrt{\frac{\text{SIR}_j}{2}}\right), \quad \text{for } j \in \{1, 2, \ldots, S\} \quad (6)$$

where

$$Q(x) = \frac{1}{\sqrt{2\pi}} \int_x^{+\infty} e^{-u^2/2}\, du.$$

Using this assumption, we have simulated the case of a dual-rate system, represented as *class lr* and *class hr* for lower and higher rate users, with two different traffic types and QoS requirements, as shown in Table I. We used a family of codes with 29 available frequencies, generated from the algorithm of Bin [10], and falling into the category of the so-called one-coincidence sequences [11]. It is characterized by the following three properties: 1) in each sequence, each frequency is used once, at most; 2) the maximum number of hits between any pair of sequences for any time shift equals one; and 3) it

[2]Hamming function

$$h(a,b) = \begin{cases} 0, & \text{if } a \neq b \\ 1, & \text{if } a = b. \end{cases}$$

TABLE I
SYSTEM PARAMETERS: DUAL RATE SYSTEM

	Lower rate	Higher rate
Processing gain	$N_{lr}=12$	$N_{hr}=6$
Transmission rate	R_{lr}=500 Mbps	R_{hr}=1 Gbps
Min. allowed SIR	$\beta_{lr}=60$	$\beta_{hr}=40$

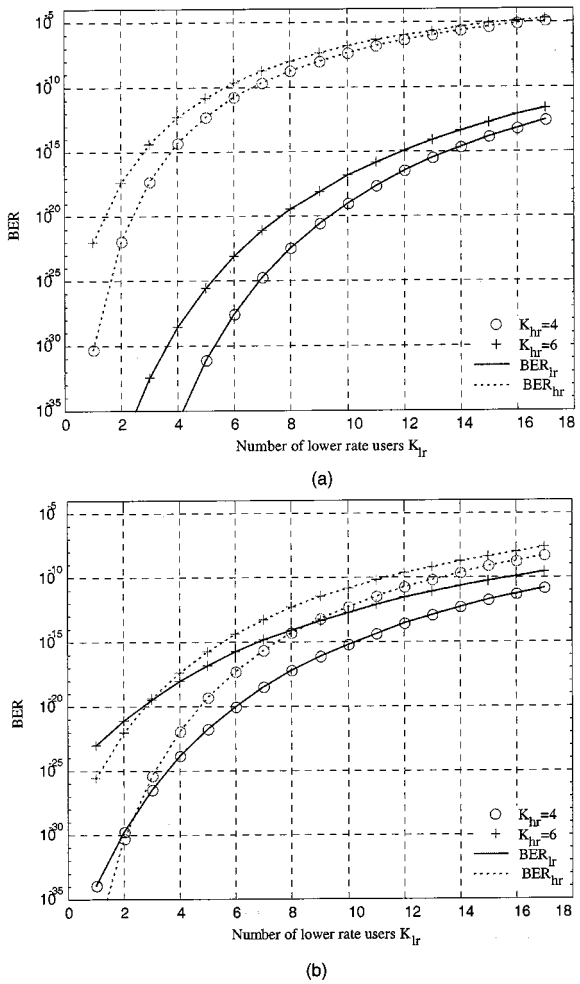

Fig. 4. BER for both classes with fixed number of higher rate users and using (a) $P^{(lr)} = P^{(hr)} = 1$, and (b) $P^{(lr)} = P^{(hr)}/2 = 0.5$.

preserves good auto- and cross-correlation properties between codes with different lengths obtained by truncating long codes [11].

Fig. 4(a) shows the BER performance for both classes using normalized equal transmission power (assuming $P = 1$), $P^{(lr)} = P^{(hr)} = 1$. It is clear that the BER for higher rate users is much higher than that for lower rate users. As mentioned before, this will lead to a wide diversity between the performances of the two classes, and the possibility of adding higher rate users will be limited for stringent QoS requirements. As shown in Fig. 4(b), when $P^{(lr)}$ is reduced to 0.5, the *class* lr bit energy is reduced, resulting in higher BER. On the other hand, the BER performance is improved for *class* hr. This improvement is due to the reduction of the MAI variance for *class* hr users.

IV. SYSTEM CAPACITY

A. Admissible Region

In this section, we establish a relation between number of users, QoS requirements, and transmission powers in each class. For simplicity, we describe the case of the two-rate system illustrated in Section III-C. We impose a minimum QoS for each rate by fixing a lower bound for the SIR, i.e., $\text{SIR}^{j}_{\min} = \beta_j$ where $j \in \{hr, lr\}$. Using (5), we obtain two inequalities for the number of users in each class.

$$K_{hr} + \frac{\alpha_{lr}}{\alpha_{hr}} \frac{\sigma^2_{hr,lr}}{\sigma^2_{hr}} \times K_{lr} \leq \tilde{K}_{hr} \tag{7}$$

$$K_{lr} + \frac{\alpha_{hr}}{\alpha_{lr}} \frac{\sigma^2_{lr,hr}}{\sigma^2_{lr}} \times K_{hr} \leq \tilde{K}_{lr} \tag{8}$$

where $\tilde{K}_{hr}$ and $\tilde{K}_{lr}$ represent the maximum number of active users in *class* hr and *class* lr when there are no *class* lr and *class* hr users, respectively. They are given by

$$\tilde{K}_{hr} = 1 + \frac{1}{\beta_{hr}} \frac{N^2_{hr}}{\sigma^2_{hr}} - \frac{\left(\sigma^2_n\right)'}{\sigma^2_{hr}} \tag{9}$$

$$\tilde{K}_{lr} = 1 + \frac{1}{\beta_{lr}} \frac{N^2_{lr}}{\sigma^2_{lr}} - \frac{\left(\sigma^2_n\right)'}{\sigma^2_{lr}}. \tag{10}$$

Before continuing, let us simulate the example given in Table I. Fig. 5(a) shows the admissible region for the case of equal power. Due to the diversity between the performances of the two classes, there is no intersection between the two regions. The achievable region is linear, and it is imposed by the condition on the higher rate users given by (7). By lowering $P^{(lr)}$, the region is wider; hence, more users can be supported from the two classes, as shown in Fig. 5(b). Although the boundary region generated by the QoS condition on lower rate users given by (8) is smaller, this will not affect the maximum allowable number of users in the system due to the overperformance experienced by this class.

The first intersection point, illustrated in Fig. 5(b), is reached between the two regions when the value of the power ratio $\bar{\alpha} = (\alpha_{lr}/\alpha_{hr})$ is

$$\bar{\alpha}_1 = \frac{\sigma^2_{lr,hr}}{\sigma^2_{lr}} \frac{\tilde{K}_{hr}}{\tilde{K}_{lr}}. \tag{11}$$

Below this value, the two regions begin to overlap, as shown in Fig. 5(c). This means that the diversity between the performances of the two classes is minimized. The overlap between the two regions is the admissible region. Our goal is to maximize this region in order to maximize the system capacity. Note the intersection point of the two regions (E), which plays an important role in defining the largest possible boundary region that can be achieved, as will be shown in Section V. If we further attenuate $P^{(lr)}$, there is a value after which the intersection between the two lines will no longer exist, as shown in Fig. 5(d). For this *class* lr power value, the power ratio between the two classes is

$$\bar{\alpha}_2 = \frac{\sigma^2_{hr}}{\sigma^2_{hr,lr}} \frac{\tilde{K}_{hr}}{\tilde{K}_{lr}}. \tag{12}$$

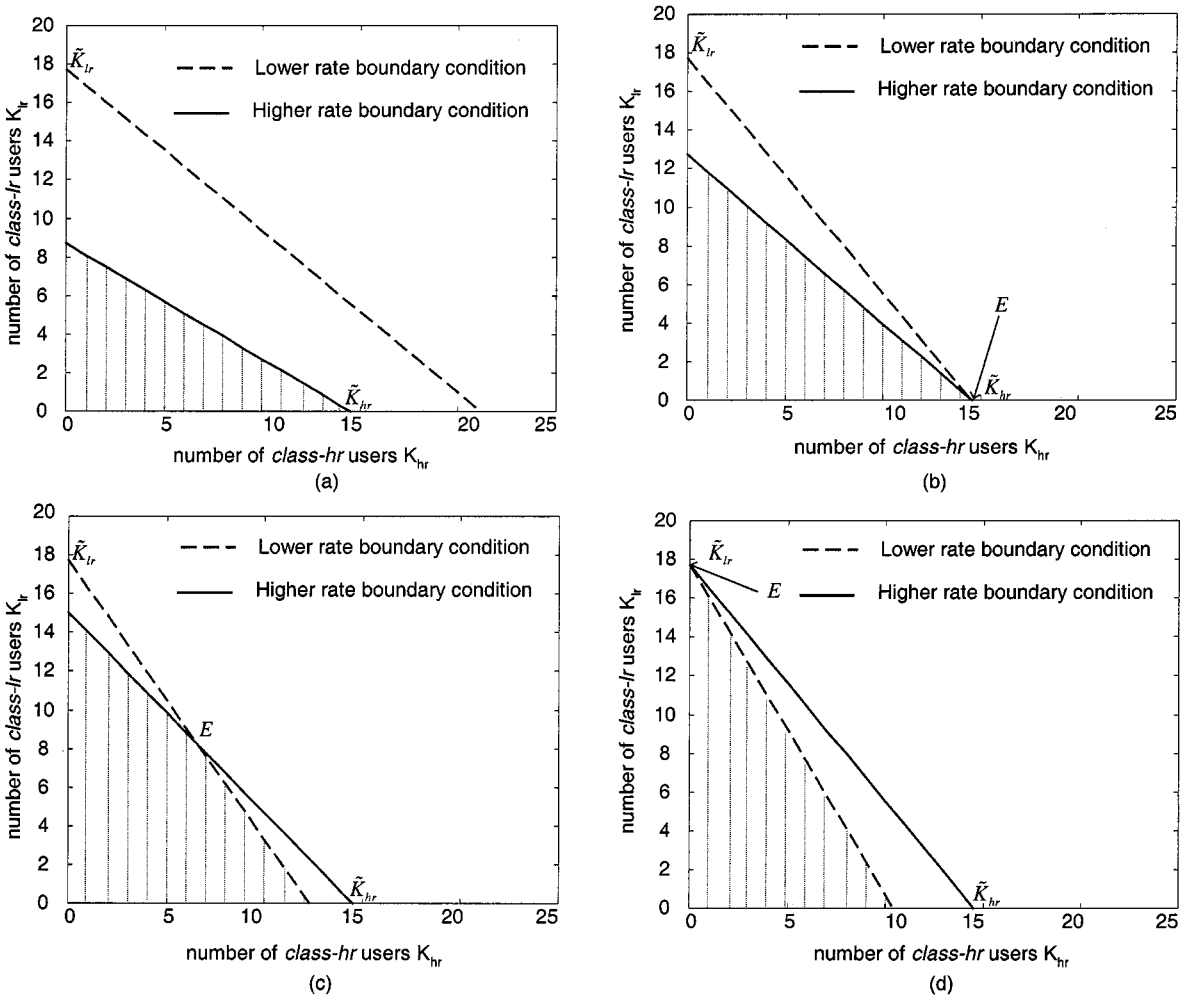

Fig. 5. Boundary limit for (K_{lr}, K_{hr}), for a given minimum $(\mathrm{SIR}_{lr}, \mathrm{SIR}_{hr})$ with $P^{(hr)} = 1$ and (a) $P^{(lr)} = 1$, (b) $P^{(lr)} = P^{(lr)}_{\max}$, (c) $P^{(lr)}_{\min} < P^{(lr)} < P^{(lr)}_{\max}$ and (d) $P^{(lr)} = P^{(lr)}_{\min}$.

Observation: It is important to mention that in an optical medium, there is a need to support a large variety of applications with very diverse traffic characteristics [1], [2]. Consequently, we observe that the optimal transmission power of each class depends on the relative values of $\tilde{K}_{hr}$ and $\tilde{K}_{lr}$. When $\tilde{K}_j \gg 1$, the "1" in (9) and (10) can be neglected. Thus, the relative value between these two parameters can be approximated by

$$\frac{\tilde{K}_{lr}}{\tilde{K}_{hr}} \approx \frac{N_{lr}^2}{N_{hr}^2} \frac{\beta_{hr}}{\beta_{lr}} \frac{\sigma_{hr}^2}{\sigma_{lr}^2}.$$

When $N_{lr} \gg N_{hr}$ and the values of β_{lr} and β_{hr} are comparable, $\tilde{K}_{lr}$ is greater than $\tilde{K}_{hr}$, as shown in Fig. 5(a). Hence, it is normal to decrease the transmission power of *class* lr users in order to increase the system admissible region. On the other hand, when $(\beta_{hr}/\beta_{lr}) \ll (N_{lr}^2/N_{hr}^2)$, $\tilde{K}_{lr}$ will be smaller than $\tilde{K}_{hr}$. This situation may happen when $\beta_{lr} \gg \beta_{hr}$, as revealed in Fig. 6(a), for $\beta_{hr} = 20$ and $\beta_{lr} = 80$. Assuming that this situation may happen in practice, the *class* hr transmission power must be decreased, compared to that of the *class* lr, in order to increase the system admissible region, as illustrated in Fig. 6(b), for a power ratio of 1.5. This procedure insures the existence of the intersection point (E) between $\bar{\alpha}_{\min} = \min\{\bar{\alpha}_1, \bar{\alpha}_2\}$ and $\bar{\alpha}_{\max} = \max\{\bar{\alpha}_1, \bar{\alpha}_2\}$ [α_1 and α_2 are given in (11) and (12), respectively] whether $\bar{\alpha}$ increased or decreased, depending on the system requirements.

B. Generalized Concept

The expression for the admissible region can be easily generalized to S classes of users operating at S different rates. The inequalities governing the system capacity for S classes are given by

$$\begin{aligned} &K_1 + d_{12}K_2 + \cdots + d_{1S}K_S \le \tilde{K}_1 \\ &d_{21}K_1 + K_2 + \cdots + d_{2S}K_S \le \tilde{K}_2 \\ &\cdot \\ &\cdot \\ &\cdot \\ &d_{S1}K_1 + d_{S2}K_2 + \cdots + K_S \le \tilde{K}_S. \end{aligned} \tag{13}$$

The coefficient d_{ij}, for $i, j \in \{1, \ldots, S\}$, is determined by $d_{ij} = (\alpha_j/\alpha_i)(\sigma_{i,j}^2/\sigma_i^2)$. The parameter $\tilde{K}_i$ denotes the maximum number of active users in *class* i when there are no active users in the system from other classes. Plotting these inequalities versus $K_1, K_2, \ldots, K_S$, yields the allowable region, bounded by an S-dimensional hyperplane of points representing

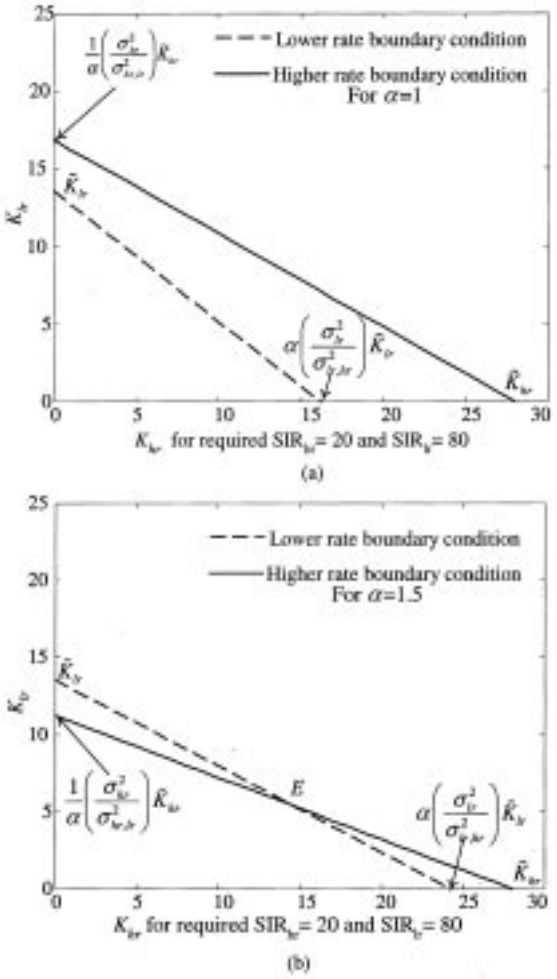

Fig. 6. Boundary limit for (K_{lr}, K_{hr}), for a given minimum $(\mathrm{SIR}_{lr}, \mathrm{SIR}_{hr})$ with $P^{(lr)} = 1$ and (a) $P^{(hr)} = 1$, (b) $P_{\min}^{(hr)} < P^{(hr)} < P_{\max}^{(hr)}$.

the maximum number of *class* i users for $i \in \{1, 2, \ldots, S\}$, and for given QoS constraints.

V. Optimization of the Power Control Function

A. System Throughput

Because each class has a different rate, the system utilization is maximized when the number of higher rate users is more than the number of lower rate users. Thus, the system throughput f is defined as the sum of the maximum allowable active users with given weights w_s for sub-*class* s. These weights represent the available rates $\{R_1, R_2, \ldots, R_S\}$, normalized by the highest rate R_S in the system. Hence, the optimization problem is presented as follows:

$$\max_{\alpha_1,\alpha_2\ldots,\alpha_S} \{f(K_1, K_2, \ldots, K_S)\} = \max_{\alpha_1,\alpha_2\ldots,\alpha_S} \left\{ \sum_{s=1}^{S} w_s K_s \right\} \tag{14}$$

with $w_s = R_s/R_S$. The constraints are

$$\mathrm{SIR}^{(s)} \geq \beta_s, \qquad \forall s \tag{15}$$

$$K_s \geq 0. \tag{16}$$

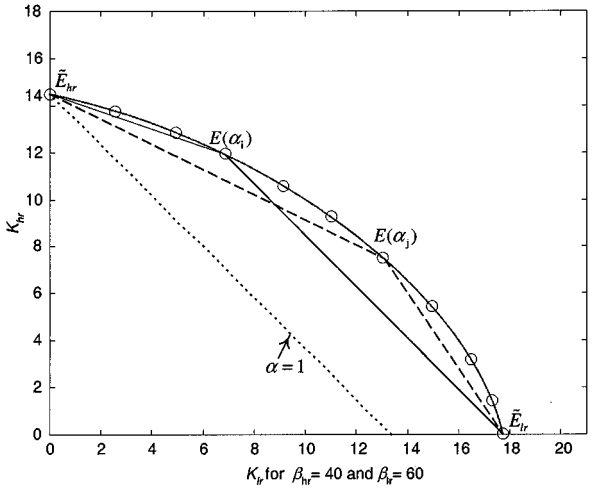

Fig. 7. The acceptance region drawn by varying the power ratio between $\alpha_{\min}$ and $\alpha_{\max}$.

B. Analytical Method

1) Two-Class System: First, consider two classes of users that have been used in previous sections, namely *class* hr and *class* lr. Equations (7) and (8) can be written in matrix form as follows:

$$\mathbf{AK} = \tilde{\mathbf{K}} \tag{17}$$

where

$$\mathbf{A} = \begin{bmatrix} 1 & \frac{\alpha_{hr}}{\alpha_{lr}} \frac{\sigma_{lr,hr}^2}{\sigma_{lr}^2} \\ \frac{\alpha_{lr}}{\alpha_{hr}} \frac{\sigma_{hr,lr}^2}{\sigma_{hr}^2} & 1 \end{bmatrix} \qquad \mathbf{K} = \begin{bmatrix} K_{lr} \\ K_{hr} \end{bmatrix}$$

$$\tilde{\mathbf{K}} = \begin{bmatrix} \tilde{K}_{lr} \\ \tilde{K}_{hr} \end{bmatrix}.$$

When $\mathrm{rank}(\mathbf{A}) = 2$, the intersection point E exists, as shown in Fig. 7. Hence, solving (17) using the coordinate of points $\tilde{E}_{lr}$ and $\tilde{E}_{hr}$ shown in Fig. 7, we obtain the following boundary limit for the power ratio:

$$\min\left\{ \left(\frac{\sigma_{hr}^2}{\sigma_{hr,lr}^2}\right)\frac{\tilde{K}_{hr}}{\tilde{K}_{lr}}, \left(\frac{\sigma_{lr,hr}^2}{\sigma_{lr}^2}\right)\frac{\tilde{K}_{hr}}{\tilde{K}_{lr}} \right\} \leq \frac{\alpha_{lr}}{\alpha_{hr}} \leq \max\left\{ \left(\frac{\sigma_{hr}^2}{\sigma_{hr,lr}^2}\right)\frac{\tilde{K}_{hr}}{\tilde{K}_{lr}}, \left(\frac{\sigma_{lr,hr}^2}{\sigma_{lr}^2}\right)\frac{\tilde{K}_{hr}}{\tilde{K}_{lr}} \right\}. \tag{18}$$

E exists in the first quadrant when $\alpha_{\min} \leq \alpha \leq \alpha_{\max}$, where $\alpha, \alpha_{\min}$, and $\alpha_{\max}$ represent values satisfying (18). Thus, by solving (17), we can write

$$K_{hr}^E(\alpha) = \frac{1}{(1 - d_{hr,lr}d_{lr,hr})}\{\tilde{K}_{hr} - d_{hr,lr}\alpha\tilde{K}_{lr}\} \tag{19}$$

$$K_{lr}^E(\alpha) = \frac{1}{(1 - d_{hr,lr}d_{lr,hr})}\left\{\tilde{K}_{lr} - \frac{d_{lr,hr}}{\alpha}\tilde{K}_{hr}\right\} \tag{20}$$

where $d_{hr,lr} = (\sigma_{hr,lr}^2/\sigma_{hr}^2), d_{lr,hr} = (\sigma_{lr,hr}^2/\sigma_{lr}^2)$ and $\alpha = \alpha_{lr}/\alpha_{hr}$. We define the weighted sum of the coordinate of E as shown in (21) at the bottom of the next page. $TH(\alpha)$ is a valid function of α because, for every power ratio α, there is

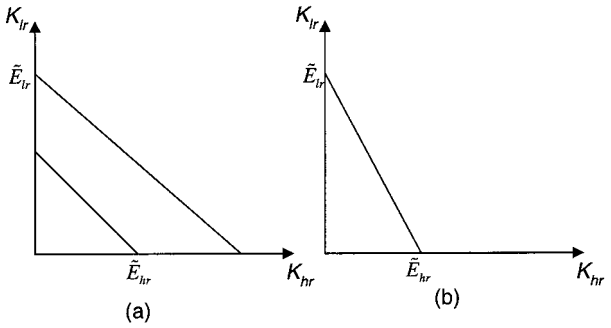

Fig. 8. The admissible region of a two-rate system with $\mathrm{rank}(\mathbf{A}) = 1$ (a) for an uncontrolled system and (b) using the optimal power ratio.

a corresponding unique value $z = TH(\alpha)$. When $\mathrm{rank}(\mathbf{A}) < 2, \det(\mathbf{A}) = 0$. For this case, the two boundary lines intersect on a line passing by $\tilde{E}_{lr}$ and $\tilde{E}_{hr}$, as shown in Fig. 8.

Proposition 1: Given that $\mathrm{rank}(\mathbf{A}) = 2$, the maximum of the throughput function $f(\alpha)$ defined in (14) is given by the maximum of the function $TH(\alpha)$. Thus

$$\max_{\alpha>0}\{f(\alpha)\} = \max_{\alpha_{\min}\le\alpha\le\alpha_{\max}}\{TH(\alpha)\}. \tag{22}$$

Therefore, the optimal power ratio α_{optimal} between the two classes is given by

$$\alpha_{\text{optimal}} = \arg\max_{\alpha_{\min}\le\alpha\le\alpha_{\max}}\{TH(\alpha)\}. \tag{23}$$

On the other hand, if $\mathrm{rank}(\mathbf{A}) < 2$, the optimal throughput is given by one of the extremes

$$\{\tilde{E}_{lr}, \tilde{E}_{hr}\} \quad \text{for } \alpha_{\text{optimal}} \in \{\alpha_{\min}, \alpha_{\max}\} \tag{24}$$

depending on whether attenuation or amplification is performed.

Proof: For a fixed power ratio α, the optimization problem defined in (14)–(16) is a linear programming problem because α is fixed and w_j is also constant. This problem is characterized by the following facts.

- The set of feasible solutions is a convex set. This convex set has a finite number of corners, which are usually referred to as extreme points.
- The set $[K_{hr}\ K_{lr}]$, which yield a specified value of the objective function, is a line. Furthermore, the lines corresponding to different values of the objective function are parallel.
- A local maximum is also the absolute (global) maximum of the objective function over the set of feasible solutions.
- If the optimal value of the objective function is bounded, at least one of the extreme points of the convex set of feasible solutions will be an optimal solution.

Thus, in our case, the global maximum is one of the extremes of the acceptance region. When we vary α' to α'', we are practically varying the acceptance region. For this new region, there is a new global maximum given by one of the extremes. Therefore, the optimization process is simplified to the search between the extreme points for every $\alpha > 0$. The extreme point that maximizes f will correspond to the optimal transmission power ratio α_{optimal}.

For each $\alpha > 0$, we define the set of extreme points $\mu = \{E_{hr}, E_{lr}, E\}$, where E is the intersection point between the two boundary lines of the admissible region if it exists. E_j, $\forall j \in \{hr, lr\}$, represents an extreme point on the jth dimension axis. E_j may vary from $(0,0)$ to the point $\tilde{E}_j$. Thus, the optimal point is either on the dimensional axis or the intersection point E. If the solution is on the jth dimension axis, then we take the maximum of E_j, which is $\tilde{E}_j$. If the solution is not on one of the axes, it will be the intersection point E for $\alpha_{\min} \le \alpha \le \alpha_{\max}$. In fact, even $\tilde{E}_j$ is an intersection point, when the lines intersect the jth dimension axis for a particular value of α. As a conclusion, the search space has now been reduced to the set of intersection points

$$\lambda = \{E(\alpha)/\alpha_{\min} \le \alpha \le \alpha_{\max}\}. \tag{25}$$

Therefore, by obtaining the maximum of $TH(\alpha)$ for $\alpha_{\min} \le \alpha \le \alpha_{\max}$, we can compute the maximum of $f(\alpha)$, which proves (22). Consequently, the optimality criterion can now be viewed as finding the α^* that maximizes the newly defined function $TH(\alpha)$ for the new boundary limits given in (18), and, thus, the proof of (23).

On the other hand, if $\mathrm{rank}(\mathbf{A}) < 2, \det(\mathbf{A}) = 0$ and the intersection point does not exists. This happens when the following equality holds true:

$$\frac{\sigma^2_{lr,hr}}{\sigma^2_{lr}} = \frac{\sigma^2_{hr}}{\sigma^2_{hr,lr}}.$$

If this expression is valid for a given family of codes, the two lines are parallel and intersect in a line when we vary α, as shown in Fig. 8. It is clear that the widest acceptance region is shown in Fig. 8(b) where attenuation is performed for the lower rate users to reach $\alpha = \alpha_{\min}$. If the acceptance region drawn from higher rate constraint is wider, the system must perform amplification for the power of the lower rate users to reach the intersection line at $\alpha = \alpha_{\max}$. Due to the fact that Fig. 8(b) is the widest possible acceptance region of the system, the optimal solution is one of the extremes $\{\tilde{E}_{lr}, \tilde{E}_{hr}\}$ for $\alpha_{\text{optimal}} \in \{\alpha_{\min}, \alpha_{\max}\}$, which proves (24). ■

$$\begin{aligned} TH(\alpha) &= K^E_{hr}(\alpha) + w_{lr}K^E_{lr}(\alpha) \\ &= \frac{1}{(1 - d_{hr,lr}d_{lr,hr})}\left\{\frac{-(d_{hr,lr}\tilde{K}_{lr})\alpha^2 + (w_{lr}\tilde{K}_{lr} + \tilde{K}_{hr})\alpha - d_{lr,hr}w_{lr}\tilde{K}_{hr}}{\alpha}\right\}. \end{aligned} \tag{21}$$

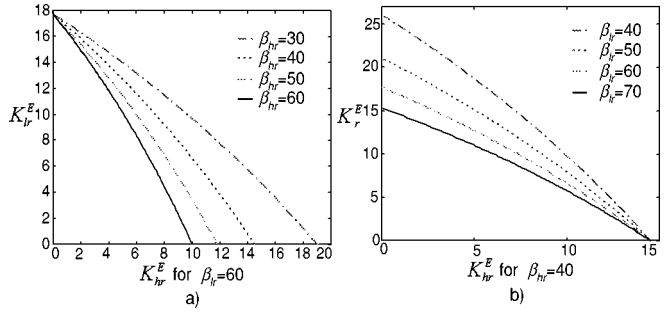

Fig. 9. The set $(K^E_{hr}(\alpha), K^E_{lr}(\alpha))$ drawn for (a) different β_{hr} requirements and (b) different β_{lr} requirements.

From this proposition, the optimization problem can be considered as a nonlinear programming problem that has linear constraints and a concave function over the nonnegative quadrant, and it can be written as

$$\max_{\alpha}\{Z = TH(\alpha)\}, \quad TH(\alpha) \text{ is concave}$$
$$\alpha_{\min} \le \alpha \le \alpha_{\max} \text{ and } \alpha \ge 0. \tag{26}$$

Because the constraints are linear and, thus, can be considered concave or convex, Kuhn–Tucker (KT) theory [12] states that a necessary and sufficient condition that TH takes on its global optimum at α^* is that there exist a λ_1^* and $\lambda_2^* \ge 0$ (Lagrange multipliers) such that

$$\frac{\partial TH(\alpha)}{\partial \alpha} - \lambda_1 + \lambda_2 = 0 \tag{27}$$
$$\lambda_1[\alpha_{\max} - \alpha] = 0 \tag{28}$$
$$\lambda_2[\alpha - \alpha_{\min}] = 0. \tag{29}$$

The values of α^*, λ_1^* and λ_2^* strongly depend on the amount of interference generated by active users and the statistics of frequency hits specified by the used family of codes. We can distinguish three cases.

i) The global maximum is between $\alpha_{\min}$ and $\alpha_{\max}$, $\lambda_1^* = \lambda_2^* = 0$ from (28) and (29). Thus, (27) yields an optimal attenuation value of

$$\alpha^* = \sqrt{\frac{d_{lr,hr} w_{lr} \tilde{K}_{hr}}{d_{hr,lr} \tilde{K}_{lr}}}. \tag{30}$$

ii) The global maximum occurs at an α greater than $\alpha_{\max}$, $\lambda_2^* = 0$ and $\alpha^* = \alpha_{\max}$. λ_1^* is computed from (27).

iii) The global maximum occurs at an α less then $\alpha_{\min}$, $\lambda_1^* = 0$ and $\alpha^* = \alpha_{\min}$. λ_2^* is also computed from (27).

Using the same family of codes applied in Section III, Fig. 9 plots the set $(K^E_{hr}(\alpha), K^E_{lr}(\alpha))$, when α varies from $\alpha_{\min}$ to $\alpha_{\max}$, for different QoS requirements of each class. Note that the search space has been transformed from a plane to a line, thus reducing the complexity of the problem and enabling us to derive an analytical solution of the optimal transmission power for each class. Fig. 9(a) shows the dependency of this line on the variations in the higher rate QoS requirements when we fix the lower rate one; on the other hand, Fig. 9(b) shows its dependency on the lower rate QoS requirements when we fix the higher rate requirements. Thus, we see the importance of the system requirements in a multimedia networks. The validity of the newly defined function $TH(\alpha)$ is demonstrated in Fig. 10(a), where we compare the analytical method versus the numerical method for different QoS requirements. By numerical function, we mean a brute-force method where we search the space $\mathbf{E}^2$ for the maximum of $f(\alpha)$. In Fig. 10(b), we plot the defined function $TH(\alpha)$ versus α. We can notice that, for $\beta_{hr} = 30$, the optimal solution is at $\alpha_{\min}$, rather than at the global maximum of the function. On the other hand, for $\beta_{hr} = 60$, the optimal solution is at α^*, given in (30).

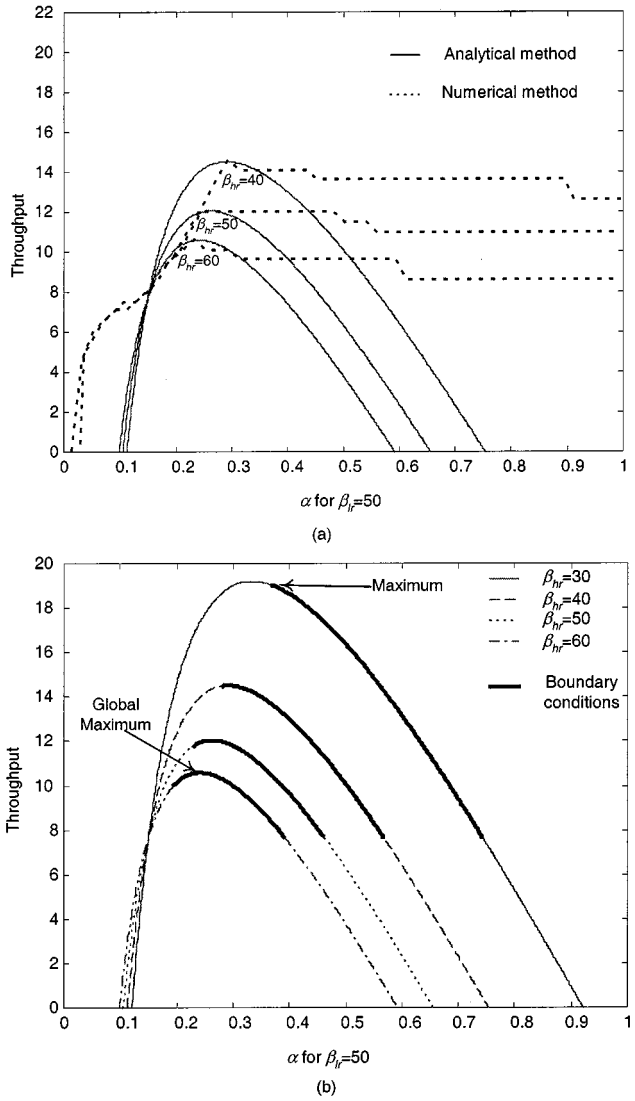

Fig. 10. Throughput versus α for several values of β_{hr} requirements with $\beta_{lr} = 50$.

2) Higher Dimensional System: In a higher dimensional system, the analysis becomes more complicated. For this reason, we begin by presenting the case of a three-rate system and then generalize the procedure to the S-class system.

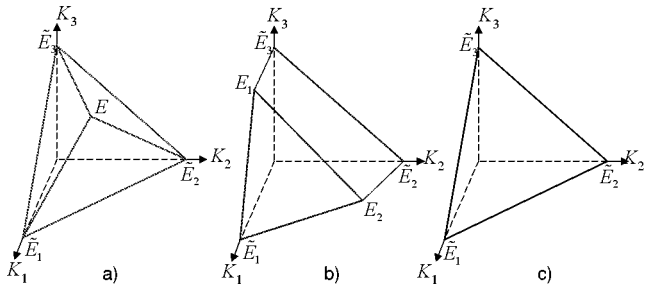

Fig. 11. The admissible region of a three-rate system with (a) $\mathrm{rank}(\mathbf{A}) = 3$, (b) $\mathrm{rank}(\mathbf{A}) = 2$, and (c) $\mathrm{rank}(\mathbf{A}) = 1$

For a three-rate system, the boundary equations can be written as in (17), with $\mathbf{A}, \mathbf{K}$ and $\tilde{\mathbf{K}}$ given by

$$\mathbf{A} = \begin{bmatrix} 1 & d_{12} & d_{13} \\ d_{21} & 1 & d_{23} \\ d_{31} & d_{32} & 1 \end{bmatrix} \qquad \mathbf{K} = \begin{bmatrix} K_1 \\ K_2 \\ K_3 \end{bmatrix}$$
$$\tilde{\mathbf{K}} = \begin{bmatrix} \tilde{K}_1 \\ \tilde{K}_2 \\ \tilde{K}_3 \end{bmatrix}$$

where $d_{ij} = (\alpha_j/\alpha_i)(\sigma_{ij}^2/\sigma_i^2)$. In this case, the problem is divided into three parts: a) $\mathrm{rank}(\mathbf{A}) = 3$; b) $\mathrm{rank}(\mathbf{A}) = 2$; and c) $\mathrm{rank}(\mathbf{A}) = 1$.

a) $\mathrm{rank}(\mathbf{A}) = 3$: The rows of $\mathbf{A}$ are linearly independent and the three planes intersect in a point E of coordinates $\mathbf{K}^E = [K_1^E \; K_2^E \; K_3^E]^T$ obtained by solving the linear set of equations in (17). If we solve (17) using the coordinate of points $\tilde{E}_1, \tilde{E}_2$ and $\tilde{E}_3$ shown in Fig. 11(a), we obtain the following boundary limits for the power ratios, which insure the existence of E in the first orthant:

$$\min\left\{\left(\frac{\sigma_j^2}{\sigma_{j,i}^2}\right)\frac{\tilde{K}_j}{\tilde{K}_i}, \left(\frac{\sigma_{i,j}^2}{\sigma_i^2}\right)\frac{\tilde{K}_j}{\tilde{K}_i}\right\} \le \frac{\alpha_i}{\alpha_j} \le \max\left\{\left(\frac{\sigma_j^2}{\sigma_{j,i}^2}\right)\frac{\tilde{K}_j}{\tilde{K}_i}, \left(\frac{\sigma_{i,j}^2}{\sigma_i^2}\right)\frac{\tilde{K}_j}{\tilde{K}_i}\right\} \quad (31)$$

where $i, j \in \{1,2,3\}$ and $j > i$. The set of extreme points is now $\mu = \{\tilde{E}_1, \tilde{E}_2, \tilde{E}_3, E\}$. This problem can be solved as in the case of the two-rate system by defining $TH(\vec{\alpha})$ as

$$TH(\vec{\alpha}) = \mathbf{W}.\mathbf{K}^E(\vec{\alpha}) = w_1 K_1^E(\vec{\alpha}) + w_2 K_2^E(\vec{\alpha}) + w_2 K_2^E(\vec{\alpha}). \quad (32)$$

b) $\mathrm{rank}(\mathbf{A}) = 2$: When $\mathrm{rank}(\mathbf{A}) = 2, \mathbf{A}^{-1}$, does not exists. In this case, there are two rows of $\mathbf{A}$ that are linearly dependent (for example, rows 2 and 3, without loss of generality). Thus, the two linearly independent planes will eventually intersect on a line, as shown in Fig. 11(b). This line will be in the first orthant, by respecting (31), and the set of extremes is given by $\mu = \{\tilde{E}_1, \tilde{E}_2, \tilde{E}_3, E_1, E_2\}$. Hence, we cannot define the throughput function based on the intersection point because it does not exist. Instead, we notice that there are two extreme points E_1 and E_2. In addition, the optimal solution will be either on the K_1oK_2 plane or on the K_1oK_3 plane; thus, the optimized system cannot support more than two classes of users. Therefore, we define two subsystems in the K_1oK_2 and K_1oK_3 planes, respectively

$$\mathbf{A}_1\mathbf{K}_1 = \tilde{\mathbf{K}}_1 \quad (33)$$
$$\mathbf{A}_2\mathbf{K}_2 = \tilde{\mathbf{K}}_2 \quad (34)$$

where $\mathbf{A}_1$ and $\mathbf{A}_2$ are submatrices generated by eliminating the third row and column and the second row and column from $\mathbf{A}$, respectively. They are given by

$$\mathbf{A}_1 = \begin{bmatrix} 1 & d_{12} \\ d_{21} & 1 \end{bmatrix} \qquad \mathbf{A}_2 = \begin{bmatrix} 1 & d_{13} \\ d_{31} & 1 \end{bmatrix}.$$

$\mathbf{K}_1, \tilde{\mathbf{K}}_1, \mathbf{K}_2$, and $\tilde{\mathbf{K}}_2$ are also given by

$$\mathbf{K}_1 = [K_1 \quad K_2] \qquad \tilde{\mathbf{K}}_1 = [\tilde{K}_1 \quad \tilde{K}_2]$$
$$\mathbf{K}_2 = [K_1 \quad K_3] \quad \tilde{\mathbf{K}}_2 = [\tilde{K}_1 \quad \tilde{K}_3].$$

Now, $\mathbf{A}_1^{-1}$ and $\mathbf{A}_2^{-1}$ exist due to the fact that these matrices are nonsingular. The solutions of the two linear systems defined in (33) and (34) give two vectors containing the coordinates of E_1 and E_2, respectively

$$\mathbf{K}^{E_1} = \mathbf{A}_1^{-1}\tilde{\mathbf{K}}_1 \text{ and } \mathbf{K}^{E_2} = \mathbf{A}_2^{-1}\tilde{\mathbf{K}}_2.$$

We define the two functions $TH_1(\vec{\alpha})$ and $TH_2(\vec{\alpha})$ based on the coordinates of E_1 and E_2 as follows:

$$TH_1(\vec{\alpha}) = \mathbf{W}_1 \cdot \mathbf{K}^{E_1}(\vec{\alpha}) = w_1 K_1^{E_1}(\vec{\alpha}) + w_2 K_2^{E_1}(\vec{\alpha}) \quad (35)$$
$$TH_2(\vec{\alpha}) = \mathbf{W}_2 \cdot \mathbf{K}^{E_2}(\vec{\alpha}) = w_1 K_1^{E_2}(\vec{\alpha}) + w_3 K_3^{E_2}(\vec{\alpha}). \quad (36)$$

c) $\mathrm{rank}(\mathbf{A}) = 1$: When $\mathrm{rank}(\mathbf{A}) = 1$, the three equations in (17) are redundant and the three planes are parallel. Therefore, the maximum acceptance region is under the plane passing by the three extreme points $\tilde{E}_1, \tilde{E}_2$, and $\tilde{E}_3$, as shown in Fig. 11(c). In this case, the optimal solution is clearly one of the extremes $\{\tilde{E}_1, \tilde{E}_2, \tilde{E}_3\}$ for $\vec{\alpha}_{\mathrm{opt}} \in \{\vec{\alpha}_{\max}, \vec{\alpha}_{\min}\}$, depending on whether attenuation or amplification is performed.

Proposition 2:

i) Given that $\mathrm{rank}(\mathbf{A}) = 3$, the maximum of the throughput function $f(\vec{\alpha})$ is given by the maximum of the function $TH(\vec{\alpha})$. Thus

$$\max_{\vec{\alpha}>0}\{f(\vec{\alpha})\} = \max_{\vec{\alpha}_{\min} \le \vec{\alpha} \le \vec{\alpha}_{\max}}\{TH(\vec{\alpha})\}. \quad (37)$$

The optimal power vector $\vec{\alpha}_{\mathrm{optimal}}$ is

$$\vec{\alpha}_{\mathrm{optimal}} = \arg \max_{\vec{\alpha}_{\min} \le \vec{\alpha} \le \vec{\alpha}_{\max}}\{TH(\vec{\alpha})\}. \quad (38)$$

ii) If $\mathrm{rank}(\mathbf{A}) = 2$, the maximum throughput is given by the maximum of the maximums of the two functions $TH_1(\vec{\alpha})$ and $TH_2(\vec{\alpha})$ defined in (35) and (36)

$$\max_{\vec{\alpha}>0}\{f(\vec{\alpha})\} = \max\left\{\max_{\vec{\alpha}_{\min} \le \vec{\alpha} \le \vec{\alpha}_{\max}}(TH_1(\vec{\alpha})), \max_{\vec{\alpha}_{\min} \le \vec{\alpha} \le \vec{\alpha}_{\max}}(TH_2(\vec{\alpha}))\right\}. \quad (39)$$

The optimal power vector $\vec{\alpha}_{\mathrm{optimal}}$ is now given by

$$\vec{\alpha}_{\mathrm{optimal}} \in \{\vec{\alpha}_{\mathrm{opt1}}, \vec{\alpha}_{\mathrm{opt2}}\} \quad (40)$$

where

$$\vec{\alpha}_{\text{opt1}} = \arg \max_{\vec{\alpha}_{\max} \le \vec{\alpha} \le \vec{\alpha}_{\max}} \{TH_1(\vec{\alpha})\}$$
$$\vec{\alpha}_{\text{opt2}} = \arg \max_{\vec{\alpha}_{\max} \le \vec{\alpha} \le \vec{\alpha}_{\max}} \{TH_2(\vec{\alpha})\}.$$

iii) If $\text{rank}(\mathbf{A}) = 1$, the maximum of $f(\vec{\alpha})$ is given by one of the extremes

$$\{\tilde{E}_1, \tilde{E}_2, \tilde{E}_3\}, \quad \text{for } \vec{\alpha}_{\text{optimal}} \in \{\vec{\alpha}_{\min}, \vec{\alpha}_{\max}\} \tag{41}$$

depending on whether attenuation or amplification is performed.

Proof: The proof of (i) and (iii) is very close to the one in proposition 1, but uses three-dimensional space. The proof of part (ii) is as follows. As shown previously, for a fixed value of the power vector $\vec{\alpha}$, the optimization problem is a linear programming problem where the solution is one of the extreme points $\{\tilde{E}_1, \tilde{E}_2, \tilde{E}_3, E_1(\vec{\alpha}), E_2(\vec{\alpha})\}$. The search space now includes two sets of extremes

$$\lambda_1 = \{E_1(\vec{\alpha}) / \vec{\alpha}_{\min} \le \vec{\alpha} \le \vec{\alpha}_{\max}\}$$
$$\lambda_2 = \{E_2(\vec{\alpha}) / \vec{\alpha}_{\min} \le \vec{\alpha} \le \vec{\alpha}_{\max}\}.$$

The set λ_1 contains $\tilde{E}_1$ and $\tilde{E}_2$ when the intersection line between the two planes passes by $\tilde{E}_1$ and $\tilde{E}_2$, respectively. On the other hand, the set λ_2 contains $\tilde{E}_1$ and $\tilde{E}_3$ when the intersection line between the two planes passes by $\tilde{E}_1$ and $\tilde{E}_3$, respectively. Therefore, the optimal solution is either in λ_1 or in λ_2. Given that the two functions $TH_1(\vec{\alpha})$ and $TH(\vec{\alpha})$, which are defined in λ_1 and λ_2, respectively, are valid functions of $\vec{\alpha}$, the maximum of each of them can be obtained along with its corresponding value of $\vec{\alpha}$. Then, the maximum of the maximum of the two functions and its corresponding power vector will represent the maximum throughput and the optimum power vector respectively, which proves (39) and (40). ∎

For a generalized S-*class* system, and using induction, it is simple to show that the expression for the power-ratio boundary condition is given by (31) with $i, j \in \{1, 2, \ldots, S\}$ and $j > i$. Again, the process is divided into three parts.

a) Full rank system: When $\text{rank}(\mathbf{A}) = S$, the inverse matrix $\mathbf{A}^{-1}$ exists. Thus, we define the weighted sum of the coordinate of E as

$$TH(\vec{\alpha}) = \mathbf{W} \cdot \mathbf{K}^E(\vec{\alpha}) = w_1 K_1^E(\vec{\alpha}) + w_2 K_2^E(\vec{\alpha}) + \ldots + w_S K_S^E(\vec{\alpha}). \tag{42}$$

In order for $TH(\vec{\alpha})$ to be a valid function of the $S(S-1)/2$ variables $(\alpha_1, \alpha_2, \ldots, \alpha_{S(S-1)/2})$ (where α_j represents the power ratio between two classes), we must ensure that, for every point $(\alpha_1, \alpha_2, \ldots, \alpha_{S(S-1)/2})$ in $\mathbf{E}^{S(S-1)/2}$, a unique number $Z = TH(\alpha_1, \alpha_2, \ldots, \alpha_{S(S-1)/2})$ can be obtained. Suppose that there are two values Z_1 and Z_2 that correspond to the point $(\alpha_1, \alpha_2, \ldots, \alpha_{S(S-1)/2})$ and are given by

$$Z_1 = \mathbf{W} \cdot \mathbf{A_1^{-1}}(\vec{\alpha}) \cdot \tilde{\mathbf{K}}, \text{ and } Z_2 = \mathbf{W} \cdot \mathbf{A_2^{-1}}(\vec{\alpha}) \cdot \tilde{K}.$$

Because the two matrices $\mathbf{A_1^{-1}}(\vec{\alpha})$ and $\mathbf{A_2^{-1}}(\vec{\alpha})$ are equal for a fixed $\vec{\alpha}$, we have $Z_1 = Z_2$. Hence, $TH(\vec{\alpha})$, defined in (42), is a valid function. Thus, the problem has been transformed to the following form:

$$\max_{\vec{\alpha}} \{Z = TH(\vec{\alpha})\} \quad (TH(\vec{\alpha}) \text{ is concave})$$
$$\vec{\alpha}_{\min} \le \vec{\alpha} \le \vec{\alpha}_{\max}, \quad \vec{\alpha} \ge 0. \tag{43}$$

For this optimization problem, KT theory [12] states that a necessary and sufficient condition that TH takes on its global optimum at $\vec{\alpha}^*$ is that there exists a vector λ^* with $\lambda_i^* \ge 0$ for $i = 1, \ldots, S(S-1)$ such that for every $j \in \{1, 2, \ldots, S(S-1)/2\}$

$$\frac{\partial TH(\vec{\alpha}^*)}{\partial \alpha_j} - \lambda_j^* + \lambda_{j+S(S-1)/2}^* = 0 \tag{44}$$
$$\lambda_j^*(\alpha_{j,\max} - \alpha_j^*) = 0 \tag{45}$$
$$\lambda_{j+S(S-1)/2}^*(\alpha_j^* - \alpha_{j,\min}) = 0 \tag{46}$$

where $\alpha_j^*, \alpha_{j,\max}$, and $\alpha_{j,\min}$ are components of the vectors $\vec{\alpha}^*, \vec{\alpha}_{\max}$, and $\vec{\alpha}_{\min}$, respectively.

b) Rank A smaller than S, a subspace approach: Suppose that $\text{rank}(\mathbf{A}) = k$ where $k < S$ and $n = S - k$; then, $n+1$ of the equations are redundant and they represent parallel hyperplanes in $\boldsymbol{E}^S$ (assumed to be the last $n+1$ equations, in this case). To generate all possible extreme points, we define $n+1$ nonsingular submatrices from $\mathbf{A}$ of order $k_2\mathbf{A}_l$, where $l \in \{k, k+1, \ldots, S\}$ stands for one of the $n+1$ linearly dependent equations. These submatrices include the $k-1$ linearly independent rows and one of the $n+1$ linearly dependent rows of $\mathbf{A}$. We drop all equations not associated with the rows of $\mathbf{A}$ appearing in each of these submatrices. Therefore, we can get the extreme point by giving zero values to the n variables not associated with the columns of $\mathbf{A}$ that appear in the kth order submatrix and then solve uniquely for the k variables associated with the columns of $\mathbf{A}$ that appear in the submatrix, because the submatrix has an inverse. The resulting S-tuple will be the coordinates of one of the extremes. In this case, the set of extreme points is $\{\tilde{E}_1, \tilde{E}_2, \ldots, \tilde{E}_k, E_k(\vec{\alpha}), \ldots, E_S(\vec{\alpha})\}$ where $E_l(\vec{\alpha})$ is obtained by

$$\mathbf{K}^{E_l} = \mathbf{A}_l^{-1} \tilde{\mathbf{K}}_l \tag{47}$$

with $\mathbf{K}^{E_l} = [K_1^{E_l} \quad K_2^{E_l} \quad \cdot \quad \cdot \quad K_{k-1}^{E_l} \quad K_l^{E_l}]^T$ and $\tilde{\mathbf{K}}_l = [\tilde{K}_1 \quad \tilde{K}_2 \quad \cdot \quad \cdot \quad \tilde{K}_{k-1} \quad \tilde{K}_l]^T$. Hence, E_l is in the first orthant when $\vec{\alpha}_{\min} \le \vec{\alpha} \le \vec{\alpha}_{\max}$. So, we can define the weighted sum of the coordinate of $\mathbf{K}^{E_l}$ as

$$TH_l(\vec{\alpha}) = \mathbf{W}_l \cdot \mathbf{K}^{E_l}(\vec{\alpha}) = w_1 K_1^{E_l}(\vec{\alpha}) + w_2 K_2^{E_l}(\vec{\alpha}) + \cdots + w_{k-1} K_{k-1}^{E_l}(\vec{\alpha}) + w_l K_l^{E_l}(\vec{\alpha}). \tag{48}$$

The optimization process can now be done separately in the lth subspace where $l \in \{k, k+1, \ldots, S\}$, using $TH_l(\vec{\alpha})$ for each of the $n+1$ subspaces.

$$\max_{\vec{\alpha}} \{Z^l = TH_l(\vec{\alpha})\} \quad (TH_l(\vec{\alpha}) \text{ is concave})$$
$$\vec{\alpha}_{\min} \le \vec{\alpha} \le \vec{\alpha}_{\max}, \quad \vec{\alpha} \ge 0. \tag{49}$$

Using KT theory for the problem defined in (49), we can calculate the maximum of $TH_l(\vec{\alpha}), Z_{\max}^l$, and its corresponding optimum power vector $\vec{\alpha}_{\text{opt}}^l$ using (44)–(46) with

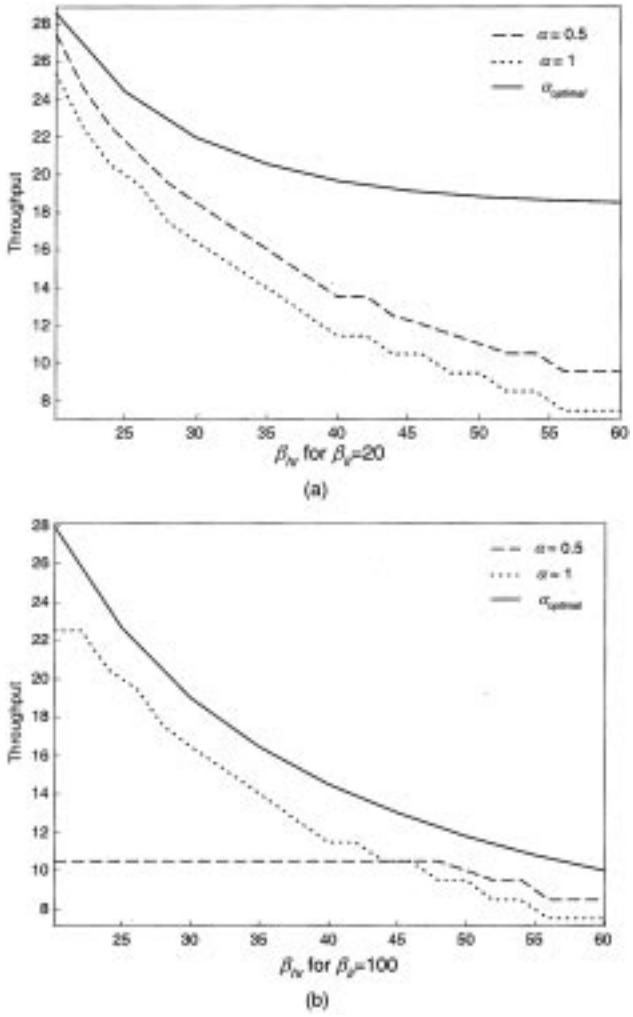

Fig. 12. Throughput versus β_{hr} requirements for optimal α (solid), $\alpha = 0.5$ (dashed), and $\alpha = 1$ (dotted) with (a) $\beta_{lr} = 20$ and (b) $\beta_{lr} = 100$.

$j \in \{1, 2, \ldots, k\}$. Thus, the maximum of the throughput function $f(\vec{\alpha})$ is given by

$$Z_{\max} = \max_{k \le l \le S} \{Z^l_{\max}\} \tag{50}$$

$$\vec{\alpha}_{\text{optimal}} \in \{\vec{\alpha}^l_{\text{opt}}\} \quad \forall l \in \{k, \ldots, S\}. \tag{51}$$

c) $\text{Rank}(\mathbf{A}) = 1$*:* The final case is when $\text{rank}(\mathbf{A}) = 1$; thus, all the hyperplanes are parallel. The widest possible region is under the hyperplane passing by the extreme points $\{\tilde{E}_1, \tilde{E}_2, \ldots, \tilde{E}_S\}$. Thus, the optimal solution is one of these extremes for $\vec{\alpha}_{\text{optimal}}$ is equal to either $\vec{\alpha}_{\min}$ or $\vec{\alpha}_{\max}$, depending on whether attenuation or amplification is performed.

VI. Numerical Results

Throughout this section, and using the two-rate system described in Section III-C, we evaluate the effectiveness of the proposed power control algorithm on the system throughput. In addition, the effects and the advantages of the new transmitters optimization method will be highlighted.

In Fig. 12, we plot the throughput versus β_{hr} for three different transmitters power settings: the conventional setting (CS) $\alpha = 1$; the equal bit energy criteria (EEC) $\alpha = 0.5$; and the proposed power control function. In the three cases, we assume

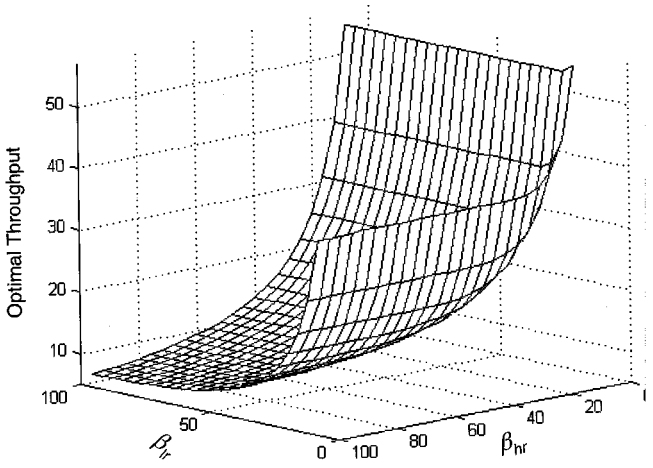

Fig. 13. Maximum throughput for different system QoS requirements scenarios.

fixed lower rate requirement β_{lr}. The most interesting case is the EEC. Intuitively, this choice of α is logical due to the fact that the lower rate codes are twice as long as the higher rate codes. When β_{lr} is low, as shown in Fig. 12(a), the system throughput increases when we attenuate the *class* lr transmission power. For this reason, when α is decreased from $\alpha = 1$ to $\alpha = 0.5$, the system throughput is increased. Thus, the intuition of imposing EEC for the two classes is rather justifiable but not optimal. Another extreme case is when we assume high β_{lr}, as shown in Fig. 12(b), for $\beta_{lr} = 100$. In this case, it can be seen that for low values of β_{hr}, the EEC introduces degradation in the system throughput. The reason is that, when $\beta_{lr} \gg \beta_{hr}$, the number of *class* lr users is smaller compared to the number of *class* hr users. Thus, the *class* hr users introduce most of the MAI. Decreasing α will further increase the interference caused by the *class* hr users on the *class* lr ones. Therefore, the system throughput will be decreased. After $\beta_{hr} = 45$, the EEC gives better results than the CS.

Nevertheless, for the two cases, the new power control strategy achieves higher system throughput than both the EEC and the conventional uncontrolled optical CDMA transmitters.

Fig. 13 shows the maximum throughput for different system requirement scenarios and using the proposed power control algorithm. It can be shown that when β_{hr} is small compared to $\beta_{lr} (\beta_{hr} < 30)$, varying β_{lr} will not significantly change the value of the maximum throughput. This is true due to the fact that when $\beta_{hr} < \beta_{lr}$, the *class* hr users dominate the system, thus affecting the system capacity more than the *class* lr users. On the other hand, when $\beta_{hr} > \beta_{lr}$, the maximum throughput will be influenced mostly by β_{lr} because the number of lower rate users that can be supported in the system is higher than the number of higher rate users. This is shown by the asymptotic behavior of the maximum throughput when β_{hr} tends to 60 for $\beta_{lr} = 30$.

The optimum power control function α is depicted in Fig. 14 versus the system requirements. Notice the importance of the QoS requirements on the choice of α. For higher values of β_{lr}, α_{lr} increases as β_{hr} becomes very small, and it can reach the level of amplification after $\beta_{hr} = 20$, as was demonstrated in the observation in Section IV. We also observe that for small

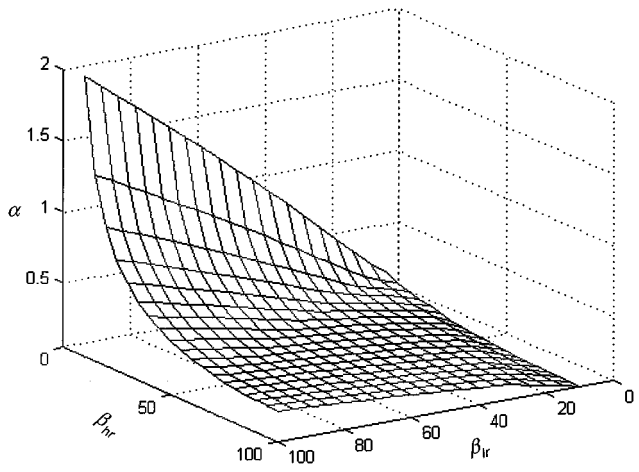

Fig. 14. Optimal α versus different system QoS requirements scenarios.

values of β_{hr}, α increases somewhat linearly as β_{lr} increases. On the other hand, there is an asymptotic behavior of α as β_{hr} and β_{lr} become very large, which leads to a constant value of the power ratio between the two classes. Observe that Fig. 14 generates the values of α that are used to calculate the optimal throughput shown in Fig. 13.

VII. Conclusion

In this paper, we have proposed an OFFH-CDMA network that insures bit-rate flexibility. Then, we have demonstrated that codes are not the only factor that must be considered in multirate optical CDMA in order to ensure a reliable system. Consequently, we have proposed using a power control algorithm for multimedia–multirate applications, using variable optical attenuators.

We have proposed a power control strategy to solve the nonlinear programming problem based on linear programming theory. Then, KT theorem was used to obtain an analytical solution for the optimal transmission power in each class. Simulations have shown that the number of active users can be efficiently increased, hence increasing the throughput. Note that the analysis presented in this paper can be extended to other optical CDMA techniques.

Future directions include extending this work to analyze a hybrid power control and coding technique, in which we will evaluate the importance of power control with respect to the used code structure. We will also study the effectiveness of power control when used with nonideal families of codes that usually contain more sequences, thus allowing a higher number of active users.

References

[1] T. D. C. Little and A. Ghafoor, "Network considerations for distributed multimedia object composition and communication," *IEEE Network Mag.*, vol. 4, pp. 32–49, Nov. 1990.

[2] J. G. Zhang, "Flexible optical CDMA networks using strict optical orthogonal codes for multimedia broadcasting and distribution applications," *IEEE Trans. Broadcast.*, vol. 45, pp. 106–115, Mar. 1999.

[3] S. Maric, O. Moreno, and C. J. Corrada, "Multimedia transmission in fiber optical LAN's using optical CDMA," *J. Lightwave Technol.*, vol. 14, pp. 2149–2153, Oct. 1996.

[4] T. Ohtsuki, "Performance analysis of direct-detection optical asynchronous CDMA systems with double optical hard-limiters," *J. Lightwave Technol.*, vol. 15, pp. 452–457, Mar. 1997.

[5] H. Fathallah, L. A. Rusch, and S. Larochelle, "Passive optical fast frequency hop CDMA communication system," *J. Lightwave Technol.*, vol. 17, pp. 397–405, Mar. 1999.

[6] L. Chen, S. Benjamin, P. Smith, and J. Sipe, "Ultrashort pulse reflection from fiber gratings: A numerical investigation," *J. Lightwave Technol.*, vol. 15, pp. 1503–1512, Aug. 1997.

[7] E. Inaty, H. M. H. Shalaby, and P. Fortier, "Multirate optical CDMA: System architecture and management," Ph.D. dissertation, Laval University, Québec, QC, Canada.

[8] A. Lempel and H. Greenberger, "Families of sequences with optimal Hamming correlation properties," *IEEE Trans. Inform. Theory*, vol. 20, pp. 90–94, Jan. 1974.

[9] J. A. Salehi and C. A. Brackett, "Code division multiple-user techniques in optical fiber networks—Part I," *IEEE Trans. Commun.*, vol. 37, pp. 824–833, Aug. 1989.

[10] L. Bin, "One-coincidence sequences with specified distance between adjacent symbols for frequency-hopping multiple access," *IEEE Trans. Commun.*, vol. 45, pp. 408–410, Apr. 1997.

[11] A. A. Shaar and P. A. Davies, "A survey of one-coincidence sequences for frequency-hopped spread spectrum systems," *IEE Proc.*, vol. 131, no. 7, pp. 719–724, Dec. 1984.

[12] L. Cooper, *Applied Nonlinear Programming for Engineers and Scientists.* Englewood, NJ: Aloray, 1974.

Elie Inaty (S'99), photograph and biography not available at the time of publication.

Hossam M. H. Shalaby (S'83–M'83–SM'99), photograph and biography not available at the time of publication.

Paul Fortier (S'79–M'82–SM'00), photograph and biography not available at the time of publication.

Leslie A. Rusch (S'91–M'94–SM'00), photograph and biography not available at the time of publication.